Contrib Mineral Petrol (1997) 130: 1–11

Rebecca A. Lange

A revised model for the density and thermal expansivity of K_2O-Na_2O-CaO-MgO-Al_2O_3-SiO_2 liquids from 700 to 1900 K: extension to crustal magmatic temperatures

Received: 2 August 1996 / Accepted: 12 June 1997

Abstract A revised model for the volume and thermal expansivity of K_2O-Na_2O-CaO-MgO-Al_2O_3-SiO_2 liquids, which can be applied at crustal magmatic temperatures, has been derived from new low temperature (701–1092 K) density measurements on sixteen supercooled liquids, for which high temperature (1421–1896 K) liquid density data are available. These data were combined with similar measurements previously performed by the present author on eight sodium aluminosilicate samples, for which high temperature density measurements are also available. Compositions (in mol%) range from 37 to 75% SiO_2, 0 to 27% Al_2O_3, 0 to 38% MgO, 0 to 43% CaO, 0 to 33% Na_2O and 0 to 29% K_2O. The strategy employed for the low temperature density measurements is based on the assumption that the volume of a glass is equal to that of the liquid at the limiting fictive temperature, T_f'. The volume of the glass and liquid at T_f' was obtained from the glass density at 298 K and the glass thermal expansion coefficient from 298 K to T_f'. The low temperature volume data were combined with the existing high temperature measurements to derive a constant thermal expansivity of each liquid over a wide temperature interval (767–1127 degrees) with a fitted 1σ error of 0.5 to 5.7%. Calibration of a linear model equation leads to fitted values of $\bar{V}_i \pm 1\sigma$ (cc/mol) at 1373 K for SiO_2 (26.86 ± 0.03), Al_2O_3 (37.42 ± 0.09), MgO (10.71 ± 0.08), CaO (15.41 ± 0.06), Na_2O (26.57 ± 0.06), K_2O (42.45 ± 0.09), and fitted values of $d\bar{V}_i/dT$ (10^{-3} cc/mol-K) for MgO (3.27 ± 0.17), CaO (3.74 ± 0.12), Na_2O (7.68 ± 0.10) and K_2O (12.08 ± 0.20). The results indicate that neither SiO_2 nor Al_2O_3 contribute to the thermal expansivity of the liquids, and that dV/dT^{liq} is independent of temperature between 701 and 1896 K over a wide range of composition. Between 59 and 78% of the thermal expansivity of the experimental liquids is derived from configurational (vs vibrational) contributions. Measured volumes and thermal expansivities can be recovered with this model with a standard deviation of 0.25% and 5.7%, respectively.

Introduction

An equation of state, or pressure-temperature-density relation, for multicomponent silicate liquids is essential for calculating changes in crystal-melt equilibria with pressure and also for evaluating the dynamics of melt segregation, ascent, and differentiation. Current models of silicate melt density applicable to magmatic compositions at crustal pressures (e.g., Lange and Carmichael 1990) are based on a combination of double-bob Archimedean density measurements to derive volume and thermal expansivity (e.g., Bockris et al. 1956; Stein et al. 1986; Lange and Carmichael 1987; Dingwell and Brearley 1988) and sound velocity measurements (e.g., Rivers and Carmichael 1987; Kress et al. 1988; Kress and Carmichael 1991; Webb and Courtial 1996) to constrain melt compressibility. One of the limitations imposed on such models is the restriction of the double-bob density measurements to superliquidus temperatures that often exceed those of magmatic melts in the crust by a few hundred degrees (Knoche et al. 1995).

For example, the bulk of the double-bob density data presented in Lange and Carmichael (1987) were obtained between 1573 and 1873 K; measurements at lower temperatures were generally prohibited by either the increasing viscosity of the liquids or the onset of crystallization. The elevated temperature range of the double-bob liquid density measurements has two consequences. First, although the precision of the density measurements themselves is excellent ($\sim$0.2%), the limited temperature interval over which they could be

R.A. Lange
Department of Geological Sciences, University of Michigan, Ann Arbor, MI 48109, USA

Editorial responsibility: T.L. Grove

made (typically 200–300 degrees) leads to derived thermal expansivities with uncertainties of ~25%. Second, and perhaps more importantly, it causes the Lange and Carmichael (1990) density model to involve a downward extrapolation in temperature when applied to crustal magmatic melts at 973–1273 K.

Therefore, in an effort to extend the available density data set for multicomponent silicate melts to significantly lower temperatures and to improve the precision and accuracy of derived thermal expansivities, the purpose of this study was to obtain low-temperature density measurements on a variety of multicomponent silicate supercooled liquids for which precise, high-temperature liquid density data already exist (Lange and Carmichael 1987). Because the sample compositions in this study were analyzed by wet chemical techniques, the volume of all sample liquids have a precision that is $< 0.3\%$. The importance of precise compositional data arises first when density measurements are converted to molar volumes and again when the partial molar properties are derived. The combination of the low and high temperature volume data allows a model equation to be derived that can be applied at both mantle and crustal magmatic temperatures.

Experimental procedure

Samples

The sixteen samples employed in this study were synthesized and wet chemically analyzed by Lange and Carmichael (1987). These samples were re-melted at 1573–1773 K and then quenched to glasses to ensure that they were completely free of bubbles and absorbed water. All sixteen samples were analyzed with a Cameca Camebax electron microprobe at the University of Michigan in order to evaluate if any measurable change in composition occurred during the re-fusion process. No change in composition could be resolved and the reported analyses in Table 1 are those obtained by Lange and Carmichael (1987).

Table 1 Composition of experimental glasses (mol%)[a]

Sample	SiO_2	Al_2O_3	MgO	CaO	Na_2O	K_2O	g.f.w.
LC-2	53.40	23.07	–	19.06	4.47	–	69.067
LC-3	53.23	5.53	–	41.24	–	–	60.749
LC-4	36.70	27.09	–	36.21	–	–	69.978
LC-6	45.21	11.64	–	43.15	–	–	63.231
LC-8	60.74	9.46	–	29.80	–	–	62.853
LC-9	61.20	9.51	28.64	0.66	–	–	58.382
LC-10	56.11	10.48	33.27	0.14	–	–	57.887
LC-11	49.02	13.07	37.82	0.09	–	–	58.073
LC-12	51.14	17.28	14.12	17.45	–	–	63.823
LC-13	46.74	15.27	15.90	22.09	–	–	62.449
LC-14	49.83	–	24.55	25.63	–	–	54.208
LC-15	47.59	–	17.12	35.29	–	–	55.285
LC-17	55.02	5.25	17.20	17.27	–	5.26	59.984
LC-18	65.84	5.60	–	–	–	28.56	72.172
LC-19	67.47	–	–	–	16.03	16.50	66.017
LC-24	59.52	–	–	30.51	–	9.97	62.263

[a] From wet chemical analyses of Lange and Carmichael (1987). Two standard deviation uncertainty in major elements (Carmichael 1985, unpublished data): SiO_2 (0.08 wt%), Al_2O_3 (0.08 wt%), MgO (0.06 wt%), CaO (0.04 wt%), Na_2O (0.04 wt%), K_2O (0.02 wt%). Errors are independent of the concentration present

Experimental strategy

The technique employed to obtain liquid volumes at the limiting fictive temperature (T_f') of each sample is illustrated in Fig. 1 and described in detail by Lange (1996). When a liquid is rapidly cooled through the glass transition interval, temperature-induced structural rearrangements become kinetically impeded and the structure of the liquid is "frozen" into the glass. The structure preserved in the glass is the equilibrium structure of the liquid at the fictive temperature, T_f. The limiting fictive temperature (T_f') can be defined as the temperature where an extrapolated first order property of the glass and the liquid are the same (Fig. 1; Scherer 1986; Moynihan 1995).

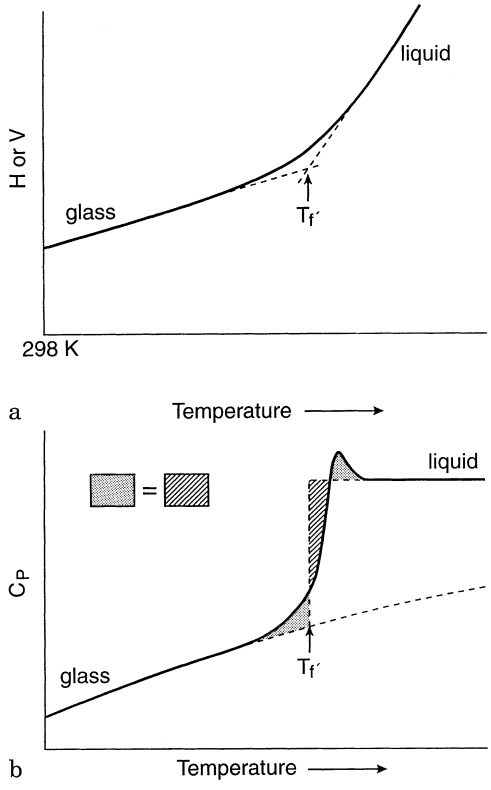

Fig. 1A A schematic diagram that illustrates how a first order thermodynamic property (e.g., enthalpy or volume) changes during cooling from a liquid to a glass. At cooling rates readily achieved in the laboratory, the liquid-glass transition does not occur abruptly at a single temperature but rather is spread out over a temperature interval. The limiting fictive temperature is defined as the intersection of the equilibrium liquid curve and the equilibrium glass curve (Scherer 1986). **B** A schematic diagram that illustrates how a second-order thermodynamic property (e.g., $C_p = dH/dT$) changes during heating of a glass (formed by cooling of a liquid as shown in diagram (A), above) to a liquid. At a heating rate of 10 K/min, the glass-liquid transition does not occur abruptly at a single temperature, but is spread out over a temperature interval because of kinetic effects. The limiting fictive temperature of the glass, however, can be defined from this curve using the area match shown in this diagram and described in Eq. 2. As noted by Moynihan (1995), any heating rate may be used (as long as thermal equilibrium is maintained during the heat capacity measurements) and need not correspond to the cooling rate used to form the glass from the liquid

From the relationship depicted in Fig. 2, the volume (or density) of a glass at room temperature will depend on how rapidly it is cooled, with slowly cooled liquids converting to higher density (lower volume) glasses. For the purpose of this study, the cooling rate of the sample liquids need not be quantified. All that is required is to measure the room temperature density (volume) of the glass as precisely as possible, followed by measurement of the glass thermal expansion up to T_f'. Glass samples of the same composition but with different cooling histories will have different room temperature densities and different T_f' values, but the volumes obtained for those glass samples at their respective limiting fictive temperatures will all be valid values for the liquid (Fig. 2).

An essential feature of the experimental strategy employed in this study is the accurate determination of T_f'. An approximation of T_f' for each glass sample is made by choosing the temperature corresponding to the onset of the rapid rise in dL/L in a dilatometry curve (Fig. 3). This is the exact approach taken by Lange (1996) in a study of the thermal expansivities of eight sodium aluminosilicate liquids. The question that arises is how well does this *approximation* of T_f' (obtained geometrically from a dilatometry curve) match the true value of T_f' (defined in Fig. 1).

A rigorous determination of T_f' can be obtained from a heating heat capacity curve because data can be collected continuously through the glass-liquid transition and into the equilibrium liquid field, whereas a comparable thermal expansivity data set cannot be obtained from a dilatometer because of viscous body forces acting on the liquid. Because T_f' is defined as the extrapolated intersection of the glass and equilibrium liquid enthalpy (H) or volume (V) vs T curves (Fig. 1A), the following area match described by Moynihan (1995) must hold for a heating heat capacity curve (Fig. 1B):

$$\int_{T \gg T_g}^{T_f'} \left(C_p^{\text{eq liq}} - C_P^{\text{glass}}\right) = \int_{T \gg T_g}^{T \ll T_g} \left(C_p^{\text{meas}} - C_p^{\text{glass}}\right) \quad (1)$$

If the heating heat capacity curve of a sample glass (with a specific composition and thermal history) has been measured through the glass-liquid transition (C_p^{meas}), and if the glass and equilibrium liquid heat capacity (C_p^{glass} and C_p^{eqliq}, respectively) curves are also known for that same sample, then T_f' can be uniquely and rigorously determined for that particular glass sample.

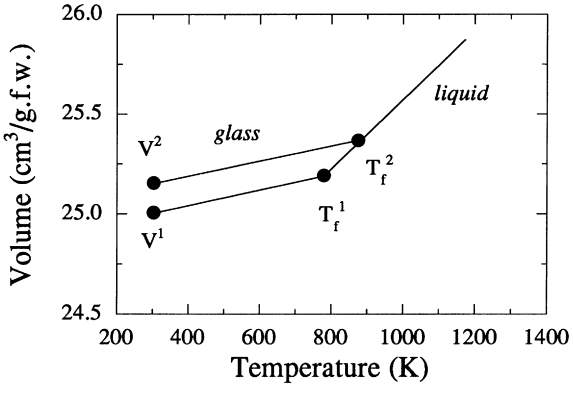

Fig. 2 A schematic diagram depicting the volume relationship of a sample liquid as it is cooled to a glass at different rates. During rapid cooling, the limiting fictive temperature will occur at a higher temperature ($T_f'^2$), leading a higher volume (lower density) glass at room temperature. During slow cooling, the limiting fictive temperature will occur at a lower temperature ($T_f'^1$), resulting in a higher density glass. The cooling history of the glass will control both the 298 K density and the glass limiting fictive temperature. Regardless of the thermal history of the glass, measurement of the density at 298 K and the thermal expansivity from 298 K to T_f' will give the volume of the liquid at T_f'

Tangeman and Lange (work submitted for publication) measured heating heat capacity curves for six of the eight sodium aluminosilicate glasses (with identical thermal histories) that were studied by Lange (1996; NAS-2, -8, -9, -10, -15 and -B), and then applied the area match of Moynihan (1995) shown in Eq. 1 to obtain values of T_f' for each of the six glasses. These determinations of T_f' were then compared to those reported by Lange (1996), which were estimated from dilatometry curves. The average deviation in T_f' determined by the two techniques is 11 degrees and the maximum deviation is 17 degrees (Tangeman and Lange 1997). In every case, but one, the estimate of T_f' from dilatometry is lower than the true value derived from calorimetry. However, a systematic underestimate of T_f' by 11 degrees contributes a negligible error to derived values of liquid volumes ($< 0.05\%$) and liquid thermal expansivities ($\leq 1\%$).

Room temperature glass density and thermal expansion measurements

Glass densities were measured at room temperature with a microbalance. First the mass of glass was measured in air (mass_{air}; five times per sample), then the mass of glass was measured below the balance while immersed in liquid toluene ($\text{mass}_{\text{toluene}}$; six times per sample). The temperature of the toluene was carefully monitored as any temperature variations between measurements can lead to systematic differences in derived densities. Sample weights in air ranged from 158 to 1204 mg. The density of each sample glass was obtained from the relationship:

$$\rho_{\text{sample}} = \frac{\rho_{\text{toluene}} \text{mass}_{\text{air}}}{\text{mass}_{\text{air}} - \text{mass}_{\text{toluene}}}, \quad (2)$$

and is reported in Table 2. Errors range from $\pm.01$ to 0.13% based on the standard deviations of the replicate mass measurements.

The linear thermal expansion coefficient of each glass sample was measured with a Perkin-Elmer TMA-7 vertical dilatometer (Lange 1996). The TMA-7 is made up of four parts: a metallic central core rod and quartz glass probe assembly, a temperature controlled LVDT (linear variable differential transformer), a linear force motor, and a furnace. Cylindrical glass samples of 3–10 mm diameter and 4–12 mm height were placed between a flat-faced quartz glass push-rod (that is attached to the metallic central core rod of the TMA) and the bottom of the quartz sample tube. Considerable care was taken to ensure that the top and bottom surfaces of the glass cylinders were as flat and parallel as possible. An applied force of 1 mN was maintained during each run; as the sample is heated (at a rate of 10 K/min), the expansion of the glass sample forces the quartz push-rod up, causing the metallic core rod to move through the LVDT, allowing the length change with temperature to be measured. This provides a measurement of the linear coefficient of thermal expansion for the glass. Replicate measurements on several glass samples indicate a reproducibility that is better than 3%. A test of the accuracy of the dilatometer is based on thermal expansion measurements on NIST standard-731 (a borosilicate glass). Thermal expansion of the NIST standard can be recovered within 7%; this error contributes $\leq 0.07\%$ error to the volumes of the samples at their respective T_f'.

Results

Density and volume of the glasses at 298 K

The density of all glasses was measured before and after each thermal expansion experiment (during which a glass is heated up to and through the glass transition interval) in order to evaluate the effect of any structural relaxation that may have occurred. For a single glass sample, this translated into three to four density replicates since the thermal expansion experiments were re-

Table 2 Measured density and volume at 298 K and T_f'

Sample	ρ(298 K) $\pm 1\sigma$ g/cm^3	Vol (298 K) cm^3/g.f.w	$\alpha^a 10^{-5}$/K	Vol (T_f') cm^3/g.f.w.^{b}	T_f' K
LC-2	2.6149 ± 0.0002	26.413	1.546	26.739	1092
LC-3	2.7962 ± 0.0047	21.725	2.173	22.081	1044
LC-4	2.8103 ± 0.0008	24.901	1.656	25.221	1070
LC-6	2.8330 ± 0.0006	22.319	2.142	22.689	1066
LC-8	2.6587 ± 0.0011	23.641	1.732	23.953	1057
LC-9	2.5692 ± 0.0008	22.724	1.178	22.934	1078
LC-10	2.6263 ± 0.0005	22.042	1.110	22.235	1087
LC-11	2.7145 ± 0.0008	21.394	1.350	21.616	1064
LC-12	2.6932 ± 0.0035	23.698	1.373	23.951	1072
LC-13	2.7567 ± 0.0003	22.654	1.624	22.934	1056
LC-14	2.8510 ± 0.0005	19.014	2.498	19.357	1013
LC-15	2.8951 ± 0.0004	19.096	2.434	19.431	1013
LC-17	2.6478 ± 0.0008	22.656	2.171	23.010	1016
LC-18	2.4426 ± 0.0006	29.547	3.540	30.145	867
LC-19	2.4791 ± 0.0008	26.629	5.072	27.179	701
LC-24	2.6405 ± 0.0015	23.580	2.872	24.040	970

[a] α–$1/V_T$ ($dV_T dT$); a constant between 298 K and the reported T_f';
[b] g.f.w. = $\sum X_i$ (molecular weight)$_i$ = oxide components

peated two to three times each. Typically, the second density measurements (after the first thermal expansion run) on all glass samples were consistently higher than the first by ~0.11%, on average. Thereafter, no resolvable density variations could be detected before and after subsequent thermal expansion experiments. This increase in glass density after the first thermal expansion run most likely reflects the effect of structural relaxation as the glass transition interval was approached. This effect can be seen in the replicate dilatometry scans for sample LC-12 in Fig. 3. As a consequence of this result, the first density determination on each glass sample was discarded and only the average of subsequent measurements was used.

The volume of each glass at 298 K was calculated from the density data and the compositional analyses, using the following equation:

$$V_{298\,\mathrm{K}}^{\mathrm{glass}} = \sum X_i (M.W.)_i / \rho_{298\,\mathrm{K}}^{\mathrm{glass}} \quad (3)$$

where X_i and $(M.W.)_i$ are the mole fraction and molecular weight of each oxide component, respectively. A propagation of the errors in $\rho_{298\mathrm{K}}^{\mathrm{glass}}$ and the wet chemical analyses leads to an uncertainty in $V_{298\mathrm{K}}^{\mathrm{glass}}$ that ranges from 0.11 to 0.24%.

Thermal expansion of glasses

Two replicate thermal expansion runs (dL/L vs temperature) are presented in Fig. 3a for sample LC-12, whereas a blow-up of the onset of the two glass transition intervals is shown in Fig. 3b. In the first dilatometry scan, the slope of dL/L with temperature (1/L dL/dT, the linear coefficient of thermal expansion) is a constant from 330 to 900 K (4.64×10^{-6} K^{-1}). Between 900 K and the onset of the rapid rise in dL/L (defined as T_f' in this study), the slope of dL/L decreases, presumably because of structural relaxation in the glass (that causes ~0.1% densification) as it approaches the glass transition interval. In the second dilatometric scan, the linear coefficient of expansion is a constant (4.72×10^{-6} K^{-1})

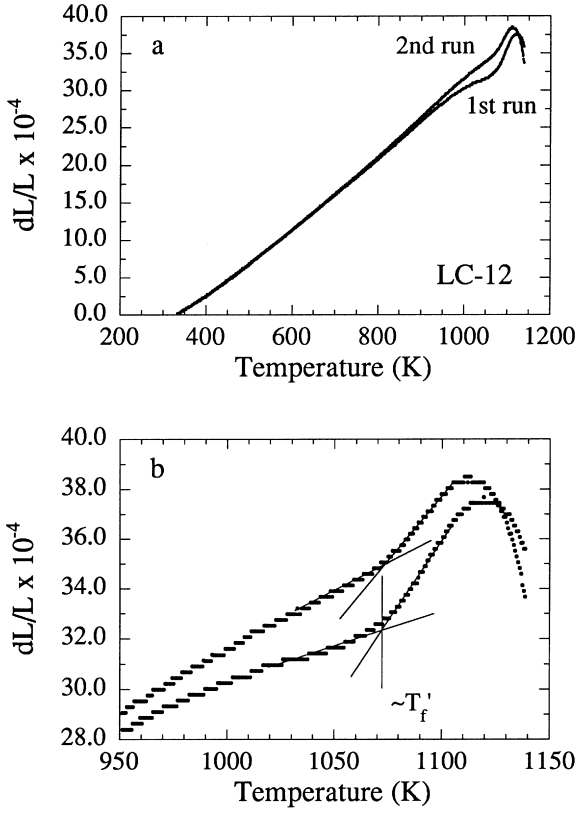

Fig. 3A Two scans of dL/L (L = length of glass cylinder) vs temperature obtained for sample LC-12 with a Perkin-Elmer TMA-7 at a heating rate of 10 K/min. The slope of the curves, between 350 and 900 K for the first run, and between 350 and 1000 K for the second run, was used to obtain the linear coefficient of thermal expansion (1/L dL/dT). The slopes are constants and the same within 1.7%. **B** The same diagram as in (**A**), but a blow-up of the two glass transition intervals. The limiting fictive temperature (T_f') is approximated from the onset of the rapid rise in the dL/L vs temperature curve at the glass transition interval

between 330 and 1000 K, and is within 1.7% of the value derived from the first scan. In this case, no evidence for any structural relaxation occurs until ~1000 K, and the same T_f' (1072 K) is observed in both scans. Moreover, the change in slope in dL/L between 1000 and 1072 K (T_f') contributes only 0.02% to the volume of the glass calculated at T_f' compared to the case when the constant linear coefficient of thermal expansion derived between 330 and 1000 K is used up to 1072 K. Therefore, for all samples, the slight change in slope as the glass transition was approached was not considered in volume calculations at T_f'.

The volume coefficient of thermal expansion, $\alpha = 1/\mathrm{V}\ \mathrm{dV}/\mathrm{d}T$, for each glass sample was obtained by multiplying the linear coefficient of thermal expansion by three. This procedure was followed for all sixteen glasses in this study; in each case, no temperature dependence to α^{glass} could be resolved (except when the glass transition interval is approached). The volume coefficient of thermal expansion (α^{glass}), combined with the 298 K glass volume, can be used to calculate the volume of each glass sample at any temperature:

$$V^{\mathrm{glass}}(T) = V^{\mathrm{glass}}_{298\ \mathrm{K}} \exp\left[\alpha^{\mathrm{glass}}(T - 298\ \mathrm{K})\right] \quad (4)$$

The volumes of all samples at their respective glass transition temperatures are reported in Table 2. A plot of volume vs temperature for both the glass and liquid phase is shown for sample LC-12 in Fig. 4.

Thermal expansivity of liquids

The low temperature liquid volume data obtained in this study at T_f' are plotted together with the high temperature liquid volume measurements of Lange and Carmichael (1987) for all sixteen samples in Fig. 5. The error bars in Fig. 5 indicate the uncertainty in the volume measurements (< 0.3%); for sample LC-19 the error is smaller than the size of the symbols. The volume vs temperature data for each liquid have been fitted to a first order polynomial; the volume equation and fitted coefficients are presented in Table 3. In every case, no temperature dependence to the thermal expansivity of the multicomponent silicate liquids can be resolved. Fitted values for $\mathrm{d}V/\mathrm{d}T^{\mathrm{liq}}$ have uncertainties that range from 0.5 to 5.7%.

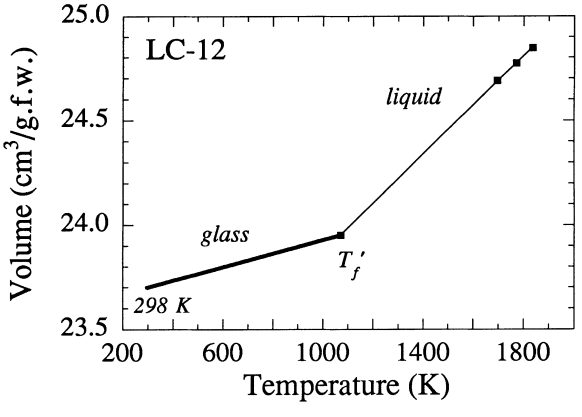

Fig. 4 Plot of volume vs temperature for LC-12 glass and liquid on the basis of the 298 K glass density measurement, the glass dilatometry, and the high temperature volume data of Lange and Carmichael (1987)

Re-calibration of a liquid volume equation

The new low-temperature liquid volume data were combined with the high temperature volume measurements on the same liquids from Lange and Carmichael (1987) to calibrate the following volume equation for K_2O-Na_2O-CaO-MgO-Al_2O_3-SiO_2 liquids:

$$V^{\mathrm{liq}}(T,X) = \sum X_i \left\{ \overline{V}_{i,T_{\mathrm{ref}}} + \mathrm{d}\overline{V}_i/\mathrm{d}T(T - T_{\mathrm{ref}}) \right\} \quad (5)$$

where X_i is the mole fraction of each oxide component, $\overline{V}_i$ is the partial molar volume of each oxide component at a reference temperature (T_{ref}) and $\mathrm{d}\overline{V}_i/\mathrm{d}T$ is the partial molar thermal expansivity of each oxide component. The regression also includes the high temperature density measurements of Bockris et al. (1956) on Na_2O-SiO_2 and K_2O-SiO_2 liquids, and of Stein et al. (1986) on eight Na_2O-Al_2O_3-SiO_2 liquids, as well as the low temperature density data of Lange (1996) on the same eight sodium aluminosilicate liquids. Because the intent was to derive values of $\overline{V}_i$ applicable to magmatic liquids, only liquids with $X_{SiO_2} \leq 0.80$ and $X_i \leq 0.50$ (where $i =$ Al_2O_3, MgO, CaO, Na_2O, K_2O) were considered.

Two separate regressions were performed with reference temperatures of 1773 and 1023 K. Derived values of $\mathrm{d}\overline{V}_i/\mathrm{d}T$ did not change between the two fits, despite the difference in T_{ref} of 750 degrees. These two T_{ref} were chosen so that fitted values of $\overline{V}_i$ and $\mathrm{d}\overline{V}_i/\mathrm{d}T$ could be directly compared to those reported by Lange and Carmichael (1987) at 1773 K, and Knoche et al. (1995) at 1023 K. Fitted values for $\mathrm{d}\overline{V}_{SiO_2}/\mathrm{d}T$ and $\mathrm{d}\overline{V}_{Al_2O_3}/\mathrm{d}T$ obtained in this study were found to be statistically indistinguishable from zero and so were dropped from the regressions. The results thus indicate that neither SiO_2 nor Al_2O_3 contribute to the thermal expansivity of these multicomponent liquids and are consistent with the previous regression of Lange and Carmichael (1987) on iron-free liquids, in which derived values for $\mathrm{d}\overline{V}_{SiO_2}/\mathrm{d}T$ and $\mathrm{d}\overline{V}_{Al_2O_3}/\mathrm{d}T$ are close to zero within 1σ error.

Calculated volumes based on the fitted values of $\overline{V}_i$ and $\mathrm{d}\overline{V}_i/\mathrm{d}T$ given in Table 4 recover the high temperature volume measurements of Bockris et al. (1956), Stein et al. (1986) and Lange and Carmichael (1987), as well as the low temperature data of Lange (1996) and this study, with a standard deviation < 0.3%. Calculated thermal expansivities for each liquid based on the results in Table 4 ($\mathrm{d}V/\mathrm{d}T^{\mathrm{liq}} = \sum X_i \times \mathrm{d}\overline{V}_i/\mathrm{d}T$) can be compared to those directly derived from the slope of the volume data vs temperature for each liquid (Fig. 5, Table 3). Calcu-

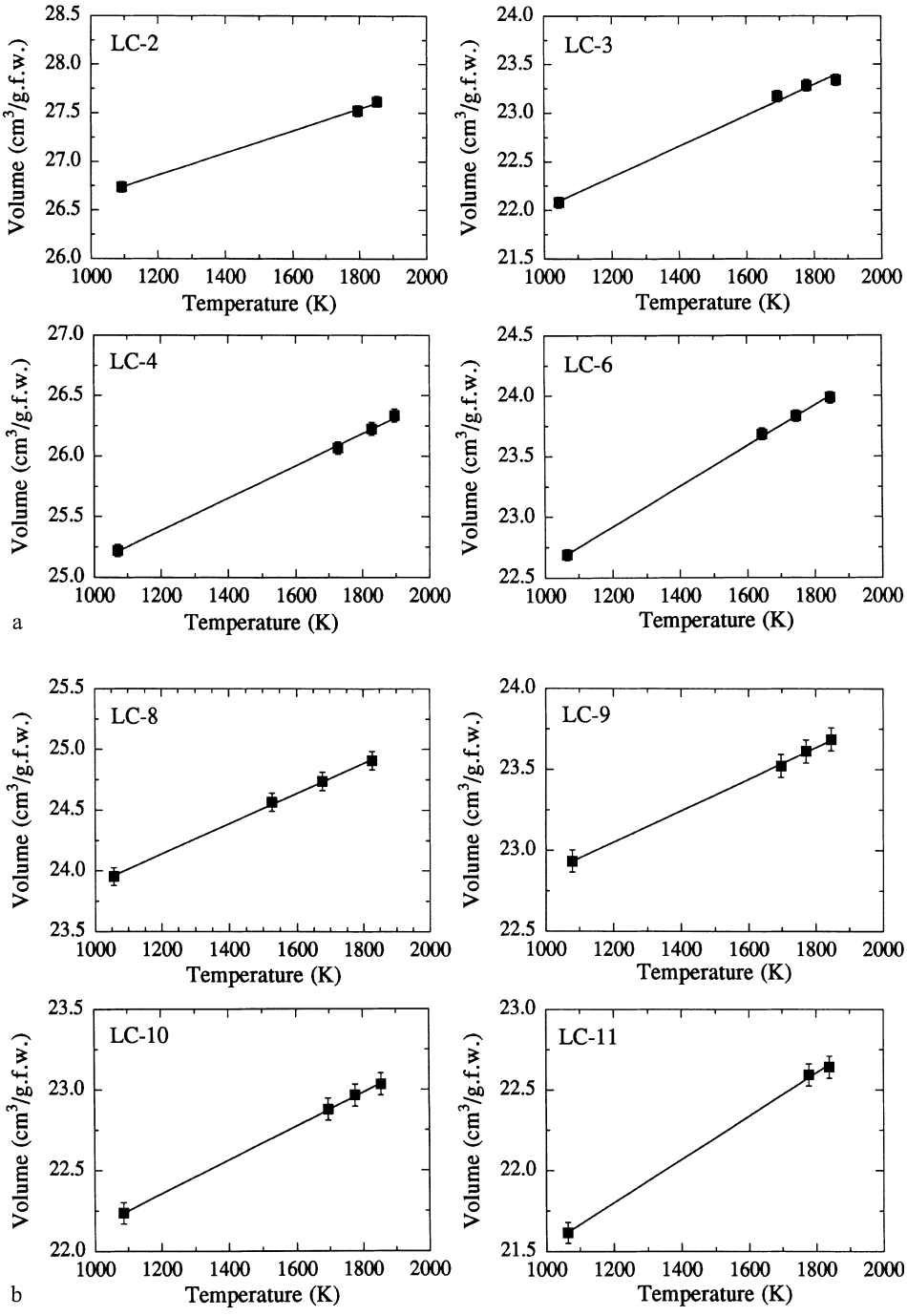

Fig. 5a–d Plots of volume vs temperature for the sixteen LC liquids; the high temperature data are from Lange and Carmichael (1987), whereas the low temperature data at T_f' are from this study. In all cases, the data can be fit with a straight line indicating no temperature dependence to the thermal expansivity (dV/dT) of each liquid. **a** LC-2, -3, -4 and -6; **b** LC-8, -9, -10, -11; **c** LC-12, -13, -14, -15; **d** LC-17, -18, -19, -24

lated values of dV/dT^{liq} are within 0–13% (5.7% on average) of the "measured" values in this study. In contrast, thermal expansivities derived from the high temperature volume measurements only (Lange and Carmichael 1987) fall within 2–42% (15.3% on average) of the predicted values. This comparison clearly illustrates the importance of the low temperature measurements for the derivation of precise silicate melt thermal expansivity data. The most important contribution of the low temperature data, however, is the calibration of a density model that extends to magmatic temperatures found in the crust.

Discussion

Configurational contributions to thermal expansivity

The thermal expansivity of silicate liquids can be divided into a vibrational and a configurational component (Richet and Neuville 1992). The vibrational component arises from an increase in the average amplitude of thermal molecular vibrations with temperature and is the sole contribution to the thermal expansivity of solids. In contrast, the configurational component is unique

Fig. 5a–d

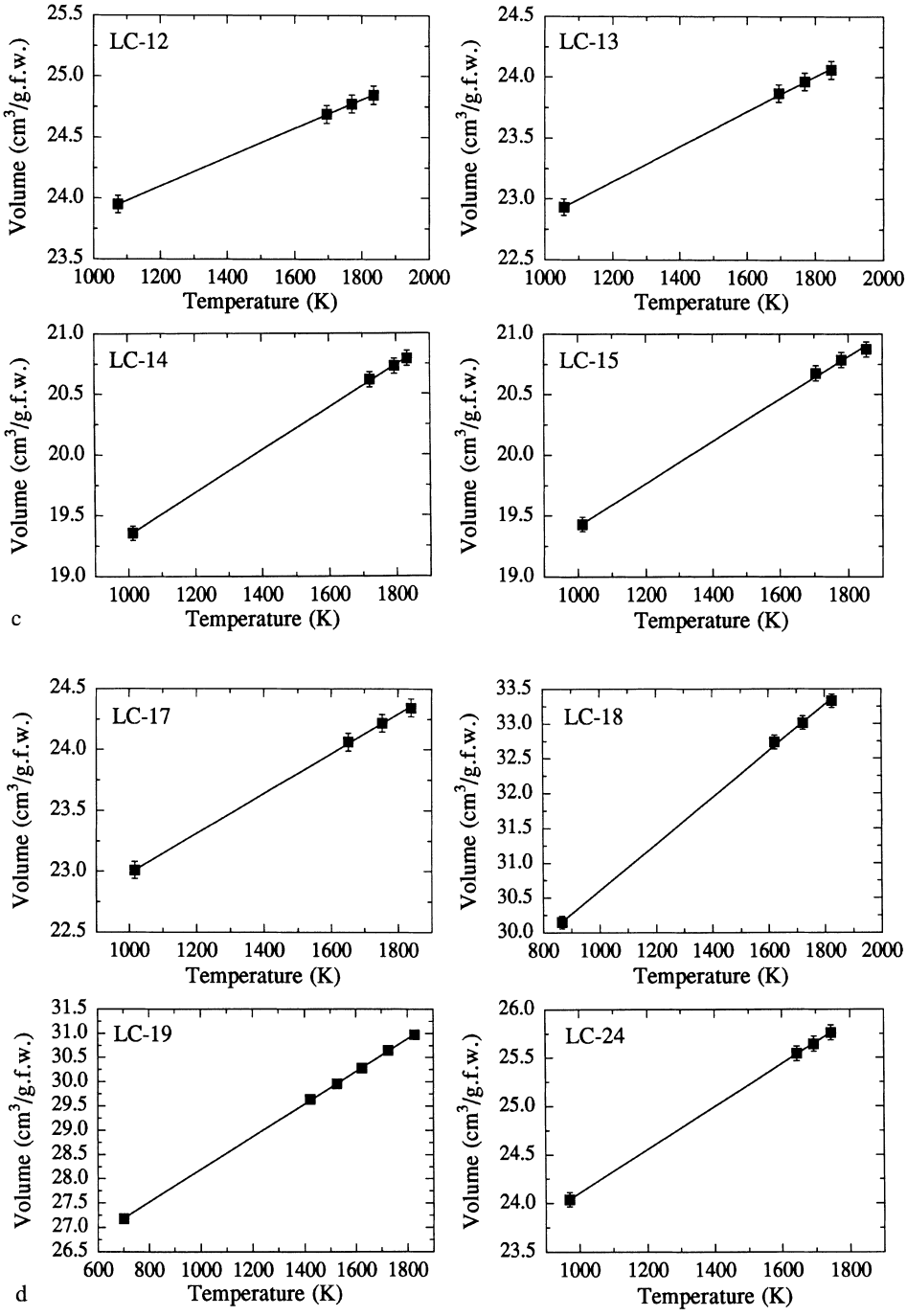

to liquids and is associated with atomic and molecular motion involved with temperature-induced structural changes (e.g., Q^n species exchange, coordination changes, structural disorder, etc.). Covalent bonds such as Si-O and Al-O undergo little, if any, expansion with temperature and therefore any contribution to the thermal expansivity from the SiO_2 and Al_2O_3 components must be configurational. However, the results of this study indicate that a configurational contribution from the SiO_2 component cannot be resolved. More surprising is that there is also no configurational contribution from the Al_2O_3 component. One possibility is that any configurational contribution to thermal expansivity from tetrahedral Al^{3+} is so dependent on the nature of the local charge-balancing cation (e.g., Mg^{2+}, Ca^{2+}, Na^+, K^+) that the effect is attributed entirely to the network modifiers in a multiple regression of Eq. 5. Nonetheless, within error, only the network modifier components contribute to the thermal expansivity of the K_2O-Na_2O-CaO-MgO-Al_2O_3-SiO_2 melts.

For each of the four network modifier components, the value for $d\overline{V}_i/dT$ has both a vibrational and a configurational component that can be distinguished based on the following relationship:

Table 3 Molar volume and thermal expansivity of liquids $V^{liquid}(T) = a + b \times 10^{-3} T$

Sample	$a(\pm 1\sigma)$	$b(\pm 1\sigma)$	T (K)	b^{vib}	b^{conf}
LC-2	25.50 ± 0.06	1.14 ± 0.04	1092–1951	0.41	0.73
LC-3	20.43 ± 0.15	1.59 ± 0.09	1044–1866	0.48	1.11
LC-4	23.79 ± 0.06	1.33 ± 0.04	1070–1896	0.42	0.91
LC-6	20.91 ± 0.05	1.67 ± 0.03	1066–1847	0.49	1.18
LC-8	22.64 ± 0.04	1.25 ± 0.03	1057–1827	0.42	0.83
LC-9	21.88 ± 0.03	0.97 ± 0.02	1078–1846	0.27	0.70
LC-10	21.10 ± 0.02	1.05 ± 0.01	1087–1855	0.25	0.80
LC-11	20.19 ± 0.07	1.34 ± 0.04	1064–1840	0.29	1.05
LC-12	22.70 ± 0.07	1.17 ± 0.01	1073–1836	0.33	0.84
LC-13	21.42 ± 0.04	1.44 ± 0.02	1056–1846	0.37	1.07
LC-14	17.56 ± 0.03	1.76 ± 0.02	1013–1833	0.48	1.28
LC-15	17.67 ± 0.08	1.75 ± 0.05	1013–1853	0.47	1.28
LC-17	21.36 ± 0.03	1.63 ± 0.02	1016–1840	0.50	1.13
LC-18	27.26 ± 0.09	3.34 ± 0.06	867–1826	1.07	2.27
LC-19	24.82 ± 0.03	3.37 ± 0.02	701–1828	1.38	1.99
LC-24	22.00 ± 0.01	2.16 ± 0.01	949–1745	0.69	1.47

Table 4 Fitted partial molar volumes and thermal expansivities

$V^{liq}(T,X) = \sum X_i \{ \bar{V}_{i,T_{ref}} + \mathrm{d}\bar{V}_i/\mathrm{d}T(T - T_{ref}) \}$

Oxide	$\bar{V}_i \pm 1\sigma$ cm^3/mol		$\mathrm{d}\bar{V}_i/\mathrm{d}T \pm 1\sigma 10^{-3}$ cm^3/mol-K	
$T_{ref} = 1773$ K				
	This study	*LC-87*[a]	*This study*	*LC-87*[a]
SiO_2	26.86 ± 0.03	26.88 ± 0.02	–	−0.33 ± 0.28
Al_2O_3	37.42 ± 0.09	37.52 ± 0.08	–	0.74 ± 0.76
MgO	12.02 ± 0.07	11.85 ± 0.06	3.27 ± 0.17	2.45 ± 0.87
CaO	16.90 ± 0.06	16.84 ± 0.05	3.74 ± 0.12	4.22 ± 0.51
Na_2O	29.65 ± 0.07	29.53 ± 0.04	7.68 ± 0.10	7.90 ± 0.46
K_2O	47.28 ± 0.10	47.10 ± 0.07	12.08 ± 0.20	12.68 ± 0.78
$T_{ref} = 1023$ K				
	This study	*KDW-95*[b]	*This study*	*KDW-95*[b]
SiO_2	26.86 ± 0.03	27.28 ± 0.19	–	0.76
Al_2O_3	37.42 ± 0.09	37.52 ± 1.90	–	−3.94
MgO	9.57 ± 0.12	10.53 ± 0.29	3.27 ± 0.17	3.93
CaO	14.10 ± 0.08	12.84 ± 0.36	3.74 ± 0.12	4.57
Na_2O	23.88 ± 0.07	21.87 ± 0.41	7.68 ± 0.10	8.68
K_2O	38.22 ± 0.12	35.18 ± 0.60	12.08 ± 0.20	12.88

[a] LC-87 = Lange and Carmichael (1987, Table 6)
[b] KDW-95 = Knoche et al. (1995, Table 5)

$$\mathrm{d}V/\mathrm{d}T^{liq} = \mathrm{d}V/\mathrm{d}T^{vib} + \mathrm{d}V/\mathrm{d}T^{conf} \quad (6)$$

In Eq. 6, $\mathrm{d}V/\mathrm{d}T^{vib}$ is the vibrational contribution to the liquid thermal expansivity and is equal to the thermal expansivity of the glass at T_f', whereas $\mathrm{d}V/\mathrm{d}T^{conf}$ is the configurational contribution to the liquid thermal expansivity and represents the abrupt jump in thermal expansivity that occurs when a glass converts to a liquid. In Table 3, experimentally derived values for both $\mathrm{d}V/\mathrm{d}T^{vib}$ and $\mathrm{d}V/\mathrm{d}T^{conf}$ are tabulated for each sample liquid. The following equations allow the vibrational and configurational contributions to $\mathrm{d}\overline{V}_i/\mathrm{d}T$ to be derived:

$$\mathrm{d}V^{vib}/\mathrm{d}T = X_i \; x \; \mathrm{d}\overline{V}_i^{vib}/\mathrm{d}T \quad (7)$$

and

$$\mathrm{d}V^{conf}/\mathrm{d}T = X_i \; x \; \mathrm{d}\overline{V}_i^{conf}/\mathrm{d}T \quad (8)$$

The fitted values ($\pm 1\sigma$) for $\mathrm{d}\overline{V}_i^{vib}/\mathrm{d}T$ and $\mathrm{d}\overline{V}_i^{conf}/\mathrm{d}T$ are given in Table 5 for the K_2O, Na_2O, CaO and MgO components. There appears to be a broad correlation between the field strength of the network modifiers and the configurational contribution to $\mathrm{d}\overline{V}_i/\mathrm{d}T$. For example, the configurational contribution ($\pm 2\sigma$) is $\sim 66(\pm 4)\%$ and $\sim 57(\pm 3)\%$ for the alkali components (K_2O and Na_2O, respectively), whereas it is as much as $\sim 70(\pm 4)\%$ and $\sim 77(\pm 7)\%$ for the alkaline earth components (CaO and MgO, respectively). Cations with even higher field strength (e.g., Fe^{3+}, Ti^{4+}) are known to contribute anomalously large configurational heat capacity to silicate liquids (Richet and Bottinga 1985; Lange and Navrotsky 1993; Tangeman and Lange 1995) and probably do so for configurational thermal expansivity as well. In the case of Ti^{4+}, the excess configurational contribution to heat capacity is inferred from in-situ Ti K-edge X-ray absorption fine structure (XAFS) spectroscopy to be related to the presence of two distinct domains within the liquid at temperatures immediately above the glass transition (Farges et al. 1996). Recent NMR studies (e.g., Brandriss and Stebbins 1988; Liu et al. 1988; Poe et al. 1992; Coté et al.

Table 5 Vibrational vs configurational $d\bar{V}_i/dT$ (10^{-3} cm^3/mol-K)[a]

X_i	$(d\bar{V}_i/dT)^{total}$	$(d\bar{V}_i/dT)^{vib}$	$(d\bar{V}_i/dT)^{conf}$	% configurational
MgO	3.26 ± 0.18	0.76 ± 0.10	2.50 ± 0.14	~77%
CaO	3.74 ± 0.13	1.14 ± 0.07	2.60 ± 0.10	~70%
Na_2O	7.75 ± 0.15	3.33 ± 0.08	4.43 ± 0.12	~57%
K_2O	11.76 ± 0.35	4.02 ± 0.19	7.74 ± 0.28	~66%

[a] Uncertainties are one standard deviation. Values for $(d\bar{V}_i/dT)^{total}$ differ (but are within 1σ error) from those given in Table 4 and derived from a fit to Eq. 5. The values in this table are the sum of the vibrational and configurational terms derived directly from fits to Eqs. 7 and 8. Table 4 provides the recommended values for density calculations

1992; Farnan and Stebbins 1990, 1994; Fiske and Stebbins 1994) have documented various temperature-induced structural changes in aluminosilicate liquids, such as silicate speciation, changes in aluminium and silicon coordination, and overall disorder. However, Stebbins (1995) argues that these dynamical features are probably *not* the dominant processes that contribute to the configurational properties of the liquid. Therefore, it is not clear what mechanisms, in detail, contribute to the configurational thermal expansivity of silicate melts. Overall, the results of this study indicate that configurational contributions account for more than half (and sometimes nearly three-quarters) of the thermal expansivity of multicomponent aluminosilicate melts.

Temperature independent liquid thermal expansivities

Recent studies by Knoche et al. (1992a, b) reported a strong temperature dependence to the thermal expansivity of several diopside-albite-anorthite ternary liquids. In contrast, the data presented in this study indicate that K_2O-Na_2O-CaO-MgO-Al_2O_3-SiO_2 liquids (non-peraluminous) have temperature-independent thermal expansivities (Fig. 5). For 14 of the 16 samples in this study, the uncertainty in dV/dT^{liq} (assumed to be independent of T) is ≤3%, whereas the other three have uncertainties < 6% (Table 3). In all cases, the first-order polynomial equations (Table 3) used to fit the volume vs temperature data in Fig. 5 recover the volume data within 0.2%, well within uncertainty of the individual measurements. There is no evidence, therefore, to support any temperature dependence to the thermal expansivity of the liquids examined in this study.

The most compelling evidence that the thermal expansivity of individual liquids is a constant over a > 1000 degree temperature interval is derived from the multiple linear regression of Eq. 5. If there were any curvature to the volume vs temperature data for individual liquids (not detected because of the absence of data at intermediate temperatures), then this temperature dependence to thermal expansivity should be evident from the quality of the fit to Eq. 5. The volume data used in the regression of Eq. 5 have a fairly uniform temperature distribution for the 16 liquids in this study combined with the eight sodium aluminosilicate liquids of Stein et al. (1986) and Lange (1996) (Fig. 6); the temperature coverage is especially good when the density data of

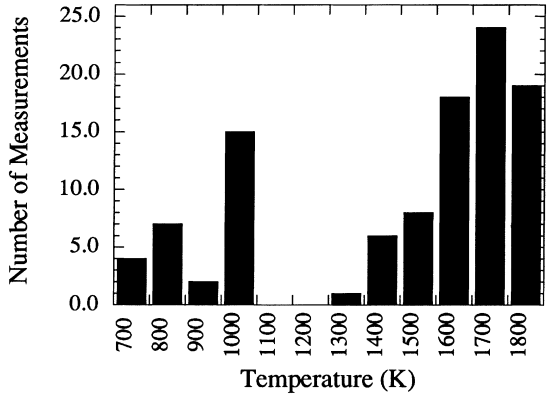

Fig. 6 Histogram of volume measurements as a function of temperature used to derive the parameters in Table 4. The distribution of temperatures is fairly uniform, with coverage between 700 and 1100 K, and between 1300 and 1900 K. Liquid volumes calculated with Eq. 4 and the fitted parameters in Table 4 recover the measured volumes within ±0.3%. The model assumes no temperature dependence to dV/dT^{liq}

Bockris et al. (1956) are considered, which include measurements between 1273–1673 K. Application of Eq. 5 allows the thermal expansivity of all liquids to be recovered within ±5.7% (on average). This result provides strong evidence that the thermal expansivity (dV/dT) of the multicomponent silicate liquids examined this study can be treated as independent of temperature for all practical purposes.

Thermal expansivity of liquid diopside

One of the samples in this study (LC-14) has a composition that corresponds to diopside ($CaMgSi_2O_6$) and thus falls within the diopside-albite-anorthite ternary system examined by Knoche et al. (1992b). In this study, the thermal expansivity of liquid diopside (LC-14) derived from the slope of the volume data with temperature (1013–1853 K) is $1.76(\pm 0.02) \times 10^{-3}$ cm^3/gram formula weight (g.f.w.)-K. This value is identical to that calculated with the model equation in Table 4 (1.76×10^{-3} cm^3/g.f.w.-K). In contrast, Knoche et al. (1992b) obtained dV/dT^{liq} values at 1053 K for two diopside supercooled liquids of slightly different composition (labeled B and GM) of 2.42×10^{-3} and 2.33×10^{-3} cm^3/g.f.w -K, respectively, which are > 32% higher than the value derived in this study.

Knoche et al. (1992b) derived the thermal expansivity of supercooled liquid diopside by equating normalized dilatometry and heat capacity curves obtained on the same diopside glass sample with an identical thermal history (see Webb et al. 1992 for a theoretical discussion of the technique). The technique is based on the premise that volume and enthalpy relaxation is equivalent through the glass-liquid transition. The large discrepancy (>32%) in the value of dV/dT^{liq} derived for diopside liquid between this study and that of Knoche et al. (1995) is substantially beyond the combined range of the errors reported in both studies (~6% and ~3%, respectively). One possible explanation is that the assumption of the equivalence of volume and enthalpy relaxation may not hold for diopside liquid.

Comparison of silicate melt density models at crustal magmatic temperatures

Calibration of a volume equation for siliceous melts that can be applied at low crustal temperatures (~973–1273 K) is of great importance to studies of intrusive granitic complexes, granitic pegmatites and the dynamics of large volume, high-silica rhyolite magma bodies. A comparison of values of $\overline{V}_i$ at 1023 K derived in this new model to the extrapolated values of $\overline{V}_i$ at 1023 K from Lange and Carmichael (1987) indicate minor, though important differences (e.g., $\overline{V}_{MgO} = 9.6$ vs 10.2, $\overline{V}_{CaO} = 14.1$ vs 13.7, $\overline{V}_{Na_2O} = 23.9$ vs 23.7 and $\overline{V}_{K_2O} = 38.2$ vs 37.8 cm^3/mol; Table 4), illustrating the necessity of the low temperature volume data to the calibration. A comparison can also be made to the model of Knoche et al. (1995), based on volume measurements on 45 haplogranitic silicate melts (17 of which fall within the K_2O-Na_2O-CaO-MgO-Al_2O_3-SiO_2 system) at their respective glass transition temperatures in a manner analogous to the procedure followed here. However, the derived values of $\overline{V}_i$ at 1023 K and $d\overline{V}_i/dT$ for the network modifier components are markedly different from those reported in this study (e.g., $\overline{V}_{MgO} = 9.6$ vs 10.5, $\overline{V}_{CaO} = 14.1$ vs 12.8, $\overline{V}_{Na_2O} = 23.9$ vs 21.9 and $\overline{V}_{K_2O} = 38.2$ vs 35.2 cm^3/mol; Table 4).

One reason for the discrepancies in $\overline{V}_i$ between the two studies may be that the MgO, CaO, Na_2O and K_2O components are not as well represented in the Knoche et al. (1995) data set as they are in the model presented here. Another reason may reside in the significantly larger compositional errors that Knoche et al. (1995) report for their sample analyses compared to those obtained in this study by wet chemistry. Knoche et al. (1995) report standard deviations in their SiO_2 analyses (obtained by ICP-AES: inductively coupled plasma-atomic emission spectrometry) that range from 0.1 to 1.4 wt% (absolute errors), whereas the standard deviation in SiO_2 by wet chemistry is ±0.04 wt% (Carmichael 1985, unpublished data). A propagation of the compositional errors (including the effects of covariance which reduce the calculated error) reported by Knoche et al. (1995, their Table 1) lead to 1σ uncertainties in their sample gram formula weights (g.f.w.) that range from 0.3 to 1.3%, with 11 of 17 samples in the K_2O-Na_2O-CaO-MgO-Al_2O_3-SiO_2 system with g.f.w. errors between 0.8 and 1.3%. From Eq. 2 it can be seen that the derived volume of any silicate melt cannot have a relative error that is less than the error in its gram formula weight, no matter how precise the density measurement. The uncertainties in composition arise again when values of $\overline{V}_i$ are derived. One advantage of this study is that all compositional analyses on the glass samples were obtained by wet chemical methods, with propagated uncertainties in the gram formula weights that are <0.1%.

Summary

A model equation for multicomponent silicate liquid densities applicable to both mantle and crustal magmatic temperatures has been calibrated between 701 and 1896 K. The results indicate that the thermal expansivities of silicate melts are independent of temperature over a wide range of composition and temperature. Perhaps more importantly, the improved precision of the $d\overline{V}_i/dT$ terms, shown to be constant over a 1200 degree interval, allows extrapolation of this model by an additional 100 degrees (in either direction) to be performed with confidence. Therefore, this model equation has the potential to be applied to melt transport at ultra high temperatures (up to 2000 K) as well as to questions regarding the dynamics of low temperature granitoid melts in the uppermost crust. The work presented here provides the basis for extending this model to include precise $d\overline{V}_i/dT$ terms for ferric and ferrous iron, as well as $\overline{V}_i$ values for the volatile components (e.g., Ochs and Lange 1997).

Acknowledgements This work was supported by NSF grants EAR-9304162 and EAR-9405768. This paper was improved by comments from Ruth Knoche, Don Dingwell and one anonymous reviewer.

References

Bockris J O'M, Tomlinson JW, White JL (1956) The structure of the liquid silicates: partial molar volumes and expansivities. Trans Faraday Soc 52:299–310

Brandriss ME, Stebbins JF (1988) Effects of temperature on the structures of silicate liquids: Si-29 NMR results. Geochim Cosmochim Acta 52:2659–2669

Coté B, Massiot D, Taullelle F, Coutures J (1992) ^{27}Al NMR spectroscopy of aluminosilicate melts and glasses. Chem Geol 96:367–370

Dingwell DB, Brearley M (1988) Melt densities in the CaO-FeO-Fe_2O_3-SiO_2 system and the compositional dependence of the partial molar volume of ferric iron in silicate melts. Geochim Cosmochim Acta 52:2815–2825

Farges F, Brown GE, Navrotsky A, Gan H, Rehr JR (1996) Coordination chemistry of Ti(IV) in silicate glasses and melts. III. Glasses and melts from ambient to high temperatures. Geochim Cosmochim Acta 60:3055–3065

Farnan I, Stebbins JF (1990) Observations of slow atomic motions close to the glass transition using 2-D ^{29}Si NMR. J Non-Cryst Solids 124:207–215

Farnan I, Stebbins JF (1994) The nature of the glass transition in a silica-rich oxide melt. Science 265:1206–1209

Fiske P, Stebbins JF (1994) The structural role of Mg in silicate liquids: a high temperature ^{25}Mg, ^{23}Na, and ^{29}Si NMR study. Am Mineral 79:848–861

Knoche R, Dingwell DB, Webb SL (1992a) Temperature-dependent thermal expansivities of silicate melts: the system anorthite-diopside. Geochim Cosmochim Acta 56:689–699

Knoche R, Dingwell DB, Webb SL (1992b) Non-linear temperature dependence of liquid volumes in the system albite-anorthite-diopside. Contrib Mineral Petrol 111:61–73

Knoche R, Dingwell DB, Webb SL (1995) Melt densities for leucogranites and granitic pegmatites: partial molar volumes for SiO_2, Al_2O_3, Na_2O, K_2O, Li_2O, Rb_2O, Ca_2O, MgO, CaO, SrO, BaO, B_2O_3, P_2O_5, F_2O_{-1}, TiO_2, Nb_2O_5, Ta_2O_5, and WO_3. Geochim Cosmochim Acta 59:4645–4652

Kress VC, Williams Q, Carmichael ISE (1988) Ultrasonic investigation of melts in the system Na_2O-Al_2O_3-SiO_2. Geochim Cosmochim Acta 52:283–293

Kress VC, Carmichael ISE (1991) The compressibility of silicate liquids containing Fe_2O_3 and the effect of composition, temperature, oxygen fugacity and pressure on their redox states. Contrib Mineral Petrol 108:82–92

Lange RA (1996) Temperature independent thermal expansivities of sodium aluminosilicate liquids between 713 and 1835 K. Geochim Cosmochim Acta 60:4989–4996

Lange RA, Carmichael ISE (1987) Densities of Na_2O-K_2O-CaO-MgO-FeO-Fe_2O_3-Al_2O_3-TiO_2-SiO_2 liquids: new measurements and derived partial molar properties. Geochim Cosmochim Acta 51:2931–2946

Lange RA, Carmichael ISE (1990) Thermodynamic properties of silicate liquids with an emphasis on density, thermal expansion and compressibility. In: Nicholls J, Russell JK (eds) Modern methods of igneous petrology. (Reviews in Mineralogy vol. 24) Mineralogical Society of America, Washington DC, pp 25–64

Lange RA, Navrotsky A (1993) Heat capacities of TiO_2-bearing silicate liquids: evidence for anomalous changes in configurational entropy with temperature. Geochim Cosmochim Acta 57:3001–3011

Liu SB, Stebbins JF, Schneider E, Pines A (1988) Diffusive motion in alkali silicate melts: an NMR study at high temperature. Geochim Cosmochim Acta 52:527–538

Moynihan CT (1995) Structural relaxation and the glass transition. In: Stebbins JF et al. (eds) Structure, dynamics and properties of silicate melts (Reviews in Mineralogy vol. 32). Mineralogical Society of America, Washington DC, pp 1–19

Ochs FA, Lange RA (1997) The partial molar volume, thermal expansivity and compressibility of H_2O in albite liquid: new measurements and an internally consistent model. Contrib Mineral Petrol (in press)

Poe BT, McMillan PF, Coté B, Massiot D, Coutures J (1992) SiO_2-Al_2O_3: in situ study by high temperature ^{27}Al NMR spectroscopy and molecular dynamic simulations. J Phys Chem 96:8220–8224

Richet P, Bottinga Y (1985) Heat capacity of aluminium-free liquid silicates. Geochim Cosmochim Acta 49:471–483

Richet P, Neuville DR (1992) Thermodynamics of silicate melts: configurational properties. Adv Phys Geochem 10:132–160

Rivers ML, Carmichael ISE (1987) Ultrasonic studies of silicate melts. J Geophys Res 92:9247–9270

Scherer GW (1986) Relaxation in glass and composites. Wiley-Interscience, New York

Stebbins JF (1995) Dynamics and structure of silicate and oxide melts: nuclear magnetic resonance studies. In: Stebbins JF et al. (eds) Structure, dynamics and properties of silicate melts (Reviews in Mineralogy vol. 32). Mineralogical Society of America, Washington DC, pp 191–246

Stein DJ, Stebbins JF, Carmichael ISE (1986) Density of molten sodium aluminosilicates. J Am Ceram Soc 69:396–399

Tangeman JA, Lange RA (1995) Measurements of viscosity and heat capacity on Na_2O-Fe_2O_3-FeO-SiO_2 melts: application of the configurational entropy theory to viscosity. Trans Am Geophys Union 76: F649

Webb SL, Courtial P (1996) Compressibility of melts in the CaO-Al_2O_3-SiO_2 system. Geochim Cosmochim Acta 60:75–86

Webb SL, Knoche R, Dingwell DB (1992) Determination of silicate liquid thermal expansivity using dilatometry and calorimetry. Eur J Mineral 4:95–104